MNRAS 000, 1–12 (2015) Preprint 25 September 2022 Compiled using MNRAS LATEX style file v3.0

Statistics and complex network for δ Scuti stars' light curves observed by *TESS*

Elham Ziaali,[1] Nasibe Alipour,[1] Hossein Safari,[1,2]★
[1]*Department of Physics, Faculty of Science, University of Zanjan, University Blvd., Zanjan, 45371-38791, Zanjan, Iran*
[2]*Observatory, Faculty of Science, University of Zanjan, University Blvd., Zanjan, 45371-38791, Zanjan, Iran*

Accepted XXX. Received YYY; in original form ZZZ

ABSTRACT

Extraction of characteristics of the complex light curve of pulsating stars is essential for stellar physics. We investigate the statistics and the complex network (Natural visibility graph and Horizontal visibility graph) properties of the high amplitude δ Scuti (HADS) and δ Sct stars light curves observed by *TESS*. We show that the probability distribution function (PDF) for the light curve of the mono-periodic HADS stars approximately follows the analytical PDF of a single-frequency sinusoidal signal that deviates at some deals due to complexity behavior. The PDF of the light curve for double mode HADS stars shows two close humps, and for multi-mode δ Sct stars, the PDFs approach a standard normal distribution with increasing the number of modes. We find that the average short path length of HADS and δ Sct light curves are a linear function of the logarithm of the network sizes, indicating the small-world and non-random properties, which also confirms by the lognormal behavior of nodes' degree distribution. The PageRank and nodes' degree distributions of HADS and δ Sct stars show different behaviors collected in two groups with decrement boundaries. The separation of two groups verifies by the scattered transitivity and average clustering coefficients of the networks. We conclude that the PDF and network approaches to the pulsating stars' light curves are helpful tools for asteroseismology.

Key words: asteroseismology – techniques: photometric – stars: variables: delta Scuti

1 INTRODUCTION

Asteroseismology is a fundamental approach for identifying and modelling stellar light curves to determine the internal structure and properties of pulsating stars (e.g Aerts et al. 2003; Christensen-Dalsgaard 2004; Baglin 2003; Chaplin et al. 2009; Aerts et al. 2010; Handler 2013; Basu & Chaplin 2017; Bowman 2017; Aerts 2021; Kurtz 2022). Space telescopes such as *CoRoT* (Baglin et al. 2009), *Kepler* (Gilliland et al. 2010) and *TESS* (Ricker et al. 2015) provide most accurate light curves for astrophysical and exoplanets investigations. Applying the time series analysis methods for the light curve of pulsating stars to investigate meaningful statistics and hidden characteristics of the system. In complex network theory, a real-world time series maps to a graph to extract the topological features of the system that do not occur in the simple analysis due to the complex behavior of the system.

Several analyses have been employed, e.g., on internal structure, mode identification, and classification for δ Sct stars (e.g., Balona & Dziembowski 2011; Uytterhoeven et al. 2011; Kahraman Aliçavuş et al. 2017; Niemczura et al. 2015; Pakštienė et al. 2018; Antoci et al. 2019; Jayasinghe et al. 2020; Bedding et al. 2020; Murphy et al. 2020; Chaplin et al. 2020; Audenaert et al. 2021; Bowman et al. 2021a; Barbara et al. 2022). The δ Sct stars are multi-periodic pulsating with intermediate masses. In the HR diagram, the δ Sct stars are at the transition region between low-mass and high-mass stars. The low-mass stars ($\leq 1M_{\odot}$) have thick convective envelopes, and high-mass stars ($\geq 2M_{\odot}$) have large convective cores and radiative envelopes. These stars have spectral types A0-F5 and pulsate in low-order pressure modes. They are in the lower part of the classical instability strip, within or just above the main sequence stars. Effective temperatures of δ Sct stars are approximately between 6500 K and 9500 K. The δ Sct stars represent various cepheid-like large amplitude radial pulsators and the non-radial multi-periodic pulsators within the classical instability strip with dominant pulsation frequencies in the range of 5-80 d^{-1} (e.g., Breger 2000; Pamyatnykh 2000; Bowman et al. 2016; Michel et al. 2017; Balona 2018; Bowman & Kurtz 2018; Pakštienė et al. 2018; Qian et al. 2018; Ziaali et al. 2019; Jayasinghe et al. 2020; Bedding et al. 2020; Hasanzadeh et al. 2021; Barac et al. 2022).

The high amplitude δ Sct stars (called HADS), are classified in population *I* of δ Sct stars with V band amplitude $\geq$ 0.3 mag and also $v \sin i \leq 30\ kms^{-1}$. However, the SX Phoenicis type of large amplitude δ Sct stars is metal-poor population II stars. The frequency spectrum of HADS stars mostly shows only one or two independent modes, which are probably radial (Breger 2000; Poretti 2003; McNamara et al. 2007; McNamara 2011; Balona et al. 2012; Balona 2016; Bowman et al. 2021b; Yang et al. 2022).

In δ Sct stars, the well-known κ mechanism, which operates in

★ E-mail: safari@znu.ac.ir

zones of partial ionization of hydrogen and helium, can drive low-order radial and nonradial modes of the low spherical degree to measurable amplitudes (opacity-driven unstable modes). In low temperature δ Sct stars, near the red edge of instability strip with substantial outer convection zones, the selection mechanism of modes with observable amplitudes could be affected by induced fluctuations of the turbulent convection. Houdek et al. (1999); Samadi et al. (2002); Antoci et al. (2011); Antoci (2014) suggested the opacity-driven unstable p modes, in which nonlinear processes limit their amplitudes, and intrinsically stable stochastically driven (solar-like) p modes can be excited simultaneously in the same δ Sct star.

The complex system methods have been widely applied for distinguishing individual and collective features in many scientific fields, such as economics (Souma et al. 2003), biology (Barabasi & Oltvai 2004), earthquakes (Baiesi & Paczuski 2004; Pastén et al. 2018; Vogel et al. 2020), and Solar physics (Daei et al. 2017; Gheibi et al. 2017; Lotfi et al. 2020; Mohammadi et al. 2021). The complex network approach could classify features with the same characteristics (e.g., the degree distribution, average clustering coefficient, transitivity, and PageRank) and quantify the complexities of dynamic systems. Graph theory is a powerful mathematical tool for exploring the characteristics of complex systems. Time series analysis based on the complex network provides information about feature structure. By mapping the time series into a natural and horizontal visibility graph, we can capture the essential characteristics of the features into distinct individual categories.

Due to light curves, categorizing the HADS and δ Sct stars is challenging. There are many reasons (e.g., superposition and amplitude modulation of modes, non-linear driving mechanisms of modes, binarity, and planets' effects) for the light curve's complexity. Here. we study the characteristics of HADS and δ Sct stars by mapping the light curves into the graph using the horizontal visibility graph (HVG) and natural visibility graph (NVG) approaches. We study the networks' local and global characteristics (nodes' degree distribution, clustering coefficients, path length, PageRank, etc.) for HADS and δ Sct stars to show the capability of complex network approaches to identifying HADS and δ Sct stars.

Section 2 explains the *TESS* data set for HADS and δ Sct stars. Section 3 discuss the methods, including the HVG and NVG algorithms to map the stellar light curves to the network. Section 4 gives results and discussions. Section 5 remarks on the important fings of this study.

2 DATA

TESS is a NASA mission and a high-precision photometric instrument (Sullivan et al. 2015; Barclay et al. 2018) and scans the sky in several sectors for millions of stars at 600-1000 nm bands (Silva Aguirre et al. 2015; Barclay et al. 2018). *TESS* observed hundreds of thousands of stars with a short cadence of 2 minutes and a long cadence of 30 minutes (Campante et al. 2016; Stassun et al. 2018; Feinstein et al. 2019) that are collected into MAST[1] in both target pixels and lightcurve files. Due to fewer data points, the complex network (Section 3.1) did not form for long cadence *TESS* observation targets. So, we queried the information and short cadence light curves of 33 (Table 1) and 40 (Table 2) HADS and δ Sct stars, respectively, by using the Python Lightkurve package (Feinstein, Montet, Foreman-Mackey, Bedell, Saunders, Bean, Christiansen, Hedges, Luger, Scolnic & Cardoso Lig).

[1] https://archive.stsci.edu

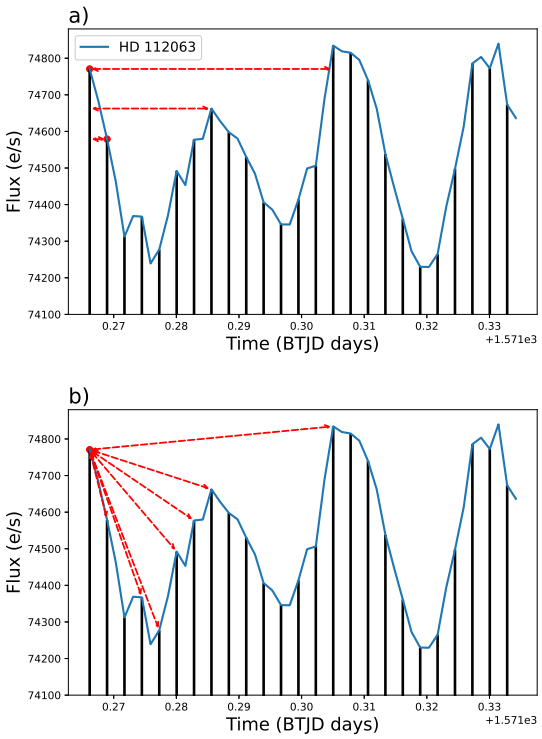

Figure 1. Horizontal visibility (a) and natural visibility (b) for the first point of light curve of HD 112063 δ Sct star. For HVG and NVG algorithms the nodes are connected based on Equations (2) and (1), respectively.

3 METHODS

3.1 Network representation of a stellar light curve

A complex network is a helpful approach to studying the characteristics of natural complex systems that evolve via complex dynamics. A complex network extract a complex system's behavior, composed of individual parts or interacting components. Then show emergent collective characteristics of the system. Natural visibility graph (NVG) and horizontal visibility graph (HVG) is among the several algorithms for building a network for a time series to study the system's characteristics (e.g., Gheibi et al. 2017; Daei et al. 2017; Najafi et al. 2020; Lotfi et al. 2020; Mohammadi et al. 2021; Taran et al. 2022; Newman 2003, 2010).

NVG and HVG are algorithms that focus on the interactions of system elements. To map a time series like a stellar light curve to a network, we consider each data point as a node (vertex), and if two elements interact, they are then connected in pairs by lines (edges or links). Figure 1 illustrates the connection of nodes (data points) for HD 112063 (TIC 9591460) light curve via the NVG and HVG algorithms.

For the HVG network for HD 112063 star, node (t_a, y_a) connects to (t_b, y_b) if an arbitrary point (t_c, y_c) such that $t_a < t_c < t_b$ satisfies the condition (Figure 1 top panel)

$$y_a, y_b > y_c. \quad (1)$$

In the NVG algorithm for HD 112063 star, we map the light curve into a network based on the visibility criterion. For two data points

(t_a, y_a) and (t_b, y_b) in the light curve have connected nodes in the graph via the criteria:

$$y_c < y_b + (y_a - y_b)\frac{t_b - t_c}{t_b - t_a} \tag{2}$$

in which (t_c, y_c) is an arbitrary data point such that $t_a < t_c < t_b$.

In the network approach, a set of local and global metrics reflect some particular features of the system. Local metrics describe individual nodes or edges, and global metrics interpret the graph as a whole. We briefly describe the nodes degree, clustering coefficient, shortest path length, and transitivity properties of an HVG network.

The node's degree of a network is one of the local metrics which measures the centrality. The node's degree is the number of edges linked to the node. Centrality shows the most influential nodes with effective connectivity through the network (Acosta-Tripailao et al. 2021). Local and average clustering coefficients are local metrics in a graph that indicate the node's tendency to cluster together and their neighbors. Transitivity is a global clustering coefficient that determines the density of triangles in a complex network. Transitivity measures the fraction of triples with their third edge served to complete the triangle. Average shortest-path length is another global metric for complex networks that define the average number of links as the shortest paths for all pairs of nodes. The Google founders developed the PageRank metric that measures the importance of every single node. The assumption is that important nodes have many in-links from essential nodes.

3.2 Power-law and lognormal distribution fits

We applied the maximum likelihood estimation in the Bayesian framework (Clauset et al. 2009; Farhang et al. 2018; Alipour et al. 2022) to obtain the fit parameters of both power-law and lognormal distributions to data. Also, applying the bootstrapping sampling, we computed the parameters' uncertainty and average (true) value for both the power law and lognormal distributions. We examined a hypothesis test based on K-S (Kolmogorov–Smirnov) statistic. The null hypothesis supposes no significant difference between the nodes' degree distribution and the lognormal/power law model. But, the alternative hypothesis assumes a substantial difference between the nodes' degree distribution and the model. We calculate a p-value to decide whether or not the lognormal/power law distribution hypothesis is plausible for our nodes' degree. A p-value more petite than the threshold of 0.1 refutes the null hypothesis showing that the lognormal/power law distribution is ruled out. We cannot deny the null for a p-value more remarkable than the threshold of 0.1.

The power-law distribution function is given by

$$\mathrm{PDF}(x, x_{\min}, \alpha) = \frac{\alpha - 1}{x_{\min}}\left(\frac{x}{x_{\min}}\right)^{-\alpha}, \tag{3}$$

where $x_{\min}$ and α are threshold and power index, respectively. This power-law or scale-free property is an essential characteristic of a self-oscillatory process that can be considered as the underlying mechanism of self-similar, self-organized, or self-organized criticality systems.

The lognormal distribution function is introduced by

$$\mathrm{PDF}(x, \mu, \sigma) = \frac{1}{\sigma\sqrt{2\pi}}\exp\left(-\frac{(\log x - \mu)^2}{2\sigma^2}\right), \tag{4}$$

where μ and σ are the scale and shape parameters, respectively. A lognormal distribution relates to a multiplicative mechanism that shows the effect of the system's independent varying parameters (Bazarghan et al. 2008; Farhang et al. 2022)

4 RESULTS AND DISCUSSIONS

In the current work, we analyzed light curves and their complex networks of δ Scuti and high amplitude δ Sct Scuti (HADS) stars observed by *TESS*. The HADS stars are mostly radial mono-periodic or double-mode pulsators, but δ Sct stars show several oscillations frequencies (multi modes). We provided a list of HADS stars, including 20 monoperiodic and 13 double-mode HADS stars. We also have 40 δ Sct Scuti stars, typically multi-periodic pulsators. We mapped the *TESS* stellar light curves of HADS and δ Sct stars into the individual networks via the HVG and NVG algorithms.

4.1 Probability distribution of light curve's flux

Figure 2 and 3 represent the PDF of light curve's flux for six HADS and six δ Sct stars respectively. We observe that the PDF of flux for mono-periodic HADS stars is similar to that of a synthetic single-frequency sinusoidal time series (Figure 4a) but deviates at some fluxes. For a single frequency sinusoidal time series $x = asin(2\pi\nu t)$, the cumulative distribution function (CDF) for a given value x_1 in the amplitude profile $(x(t))$ is introduced by,

$$\begin{aligned} \mathrm{CDF}_{\mathrm{sine}}(x < x_1) &= \mathrm{CDF}_{\mathrm{sine}}(\arcsin(2\pi\nu t) < x_1), \\ &= \mathrm{CDF}_{\mathrm{sine}}(2\pi\nu t < \arcsin(x_1/a)), \\ &= \frac{\arcsin(x_1/a) + \frac{\pi}{2}}{\pi}. \end{aligned} \tag{5}$$

where a and ν are arbitrarily amplitude and frequency of a sinusoidal time series, respectively Using Equation 5, the PDF is given by

$$\mathrm{PDF}_{\mathrm{sine}} = \frac{1}{\pi\sqrt{1 - x_1^2/a^2}}. \tag{6}$$

The PDF of amplitude profiles for a superposition of two sinusoidal signals (with random frequencies. phases, and amplitudes) deviates from the PDF of single mode signal (Figure 4b). The PDF of amplitude profiles for the superposition of six sinusoidal signals tended to have a normal-like distribution (Figure 4c) and deviated from standard normal at some bins. For a signal generated by a superposition of several modes, the PDF of amplitudes approaches a standard normal distribution (Figure 4d). The flux PDF of mono-periodic and dual-mode HADS stars (Figure 2) are close to the PDF of single frequency signal and superposition of two signals (Figure 4a and b). We examined the effect of noises (white and red noises) on the PDF and CCDF of flux for synthetic time series. The PDF and CCDF of amplitudes for artificial time series are less sensitive to different levels of noise. More investigations on observational light curves via the denoising methods require addressing the effect of the noises on the statistical behavior of light curves.

As we observe in Figure 3, the flux distribution of six δ Sct stars is likely to follow the normal distribution that slightly deviates at some fluxes. The deviation of PDF for observational flux for mono-periodic HADS and multi frequencies δ Scuti stars from analytical and simulated PDFs may depend on some essential factors. Some factors like noise and background (Lund et al. 2021), harmonics of main modes and binarity or having exoplanets and companions (Herrero et al. 2011; Liakos & Niarchos 2017; Lee et al. 2020; Kahraman Aliçavuş et al. 2022), may change the flux and the PDF distribution. The generative mechanism, e.g., κ mechanism (Eddington 1919; Cox 1963) and stochastic mechanism (Houdek et al. 1999; Samadi et al. 2002; Antoci et al. 2011; Antoci 2014; Antoci et al. 2014) behind the pulsating may produce the stochastic periodic signal that deviates from regular sinusoidal signals. More adequate investigations

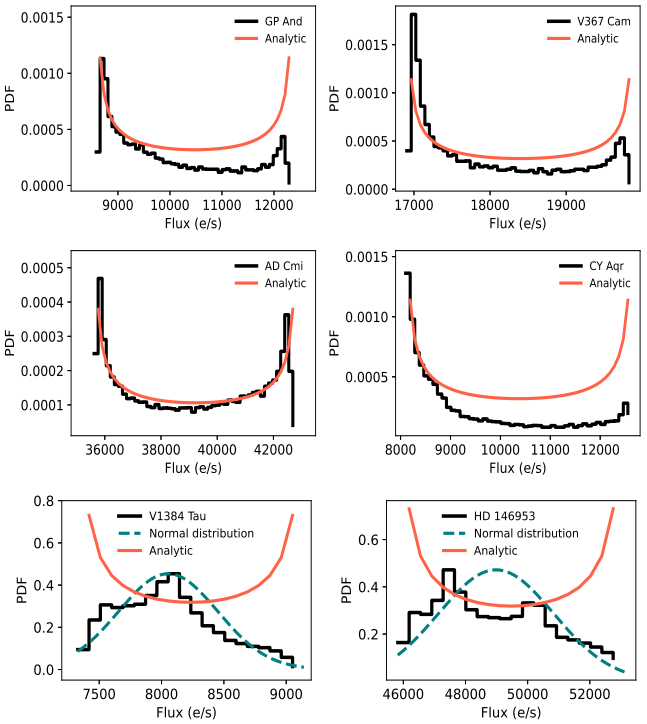

Figure 2. Probability distribution function (PDF) of light curve's flux for six stars including four mono-periodic (GP And, V367 Cam, AD Cmi, and CY Aqr) and two double-modes (V1384 Tau and HD 146953) HADS stars. The red curve represents the analytic PDF of a synthetic single-mode sinusoidal signal. The PDF of double-mode HADS deviates from the analytic PDF of a synthetic single-mode sinusoidal signal and tends to have the normal-like PDF. The normal standard distribution represents by a blue-dashed line.

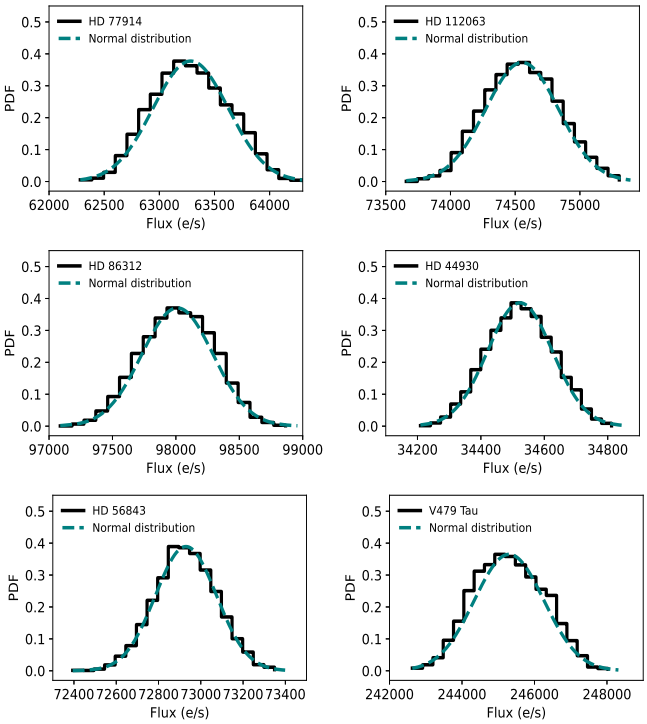

Figure 3. PDF (blue line) of light curve's flux for six multi modes δ Sct stars (HD 77914 (TIC 975071), HD 112063 (TIC 9591460), HD 86312 (TIC 26957587), HD 44930 (TIC 34737955), HD 56843 (TIC 387235455), and V479 Tau (TIC 459908110)) and normal standard distribution (blue dashed line).

are required to explore the effect of such factors on the stellar light curves.

Figure 5 shows the complementary cumulative distribution function (CCDF) for the light curves of HADS (red lines) and δ Sct (blue lines) stars, which observed two different convex and concave behaviors for CCDF curves of HADS and stars. CCDF for HADS stars almost shows the concave behavior for all fluxes, but CCDF for δ Sct stars with convexity behavior and changes to the concave behavior. The RX Cae, V353 Vel, TIC 448892817, and GW Dra are δ Sct samples (Rodríguez et al. 2000; Rucinski 2007; Chang et al. 2013; Hasanzadeh et al. 2021; Barac et al. 2022) which the CCDF of their light curves shows slightly different behavior of δ Sct stars. This ambiguity for V353 Vel (TIC 106886169) star might come from binarity (W UMa type) nature (Pribulla et al. 2003; Liakos & Niarchos 2017).

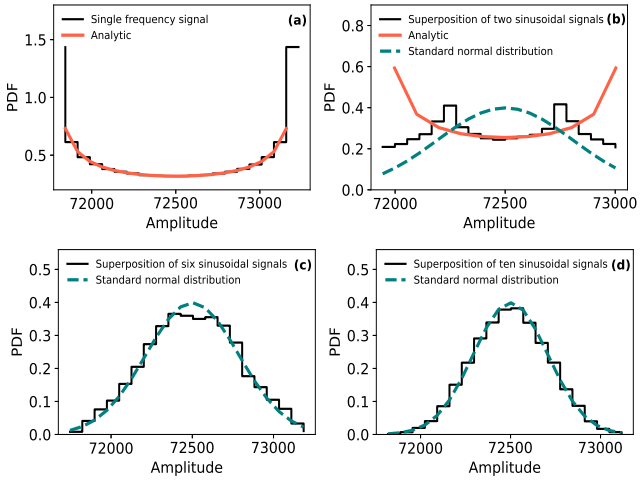

Figure 4. PDF (black line) of synthetic time series for a single sinusoidal (a), superposition of two sine signals (b), six sine signals (c), and ten sine signals (d). The analytic PDF (red line) for a single sine signal (Equation 6 and normal standard distribution (blue dashed line).)

4.2 Complex network analysis

We applied the HVG and NVG algorithms to investigate the characteristics of 33 and 40 HADS and δ Sct stars, respectively. Due to different algorithms of network structure for HVG and NVG, we represent the results for key metrics of each algorithm. Some network properties in both HVG and NVG algorithms for HADS and δ Sct stars show similar behavior, so we presented the results for one of the algorithms. Also, for some metrics without simple interpretable behavior, we ignored the analysis for those metrics.

Figure 6 represents the average shortest path length for the HVG network of GP And (HADS) and HD 113211 (δ Sct) that compared with the equivalent random network (Luque et al. 2009). As shown in the figure, the average shortest path length network for both stars has deviated from the random network. The linear dependency of the average shortest path length to the logarithm of network size for both cases indicated the small-world behavior of networks. We observed similar behavior for all target stars of Tables 1 and 2. The small world behavior for a HADS or a δ Sct star network shows that the high peaks

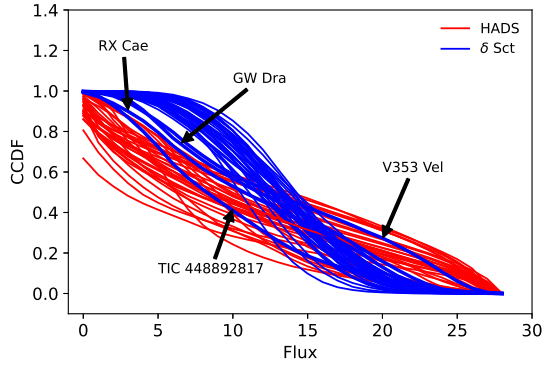

Figure 5. CCDF of flux for HADS (red lines) and δ Sct (blue lines) stars. The CCDF of light curves for RX Cae, V353 Vel, TIC 448892817, and GW Dra are samples that show different behavior of δ Sct stars.

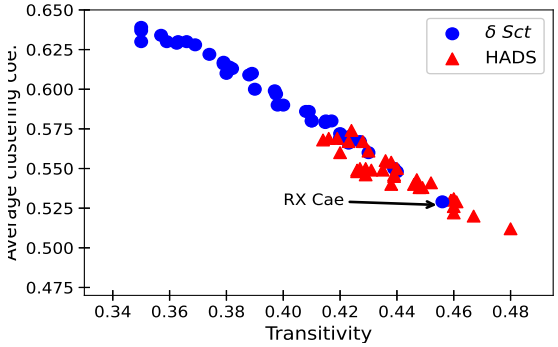

Figure 7. Scatter plot of the transitivity versus average local clustering coefficient for HVG network of δ Sct (blue circles) and HADS (red triangles) stars. The black arrow indicates δ Sct RX Cae.

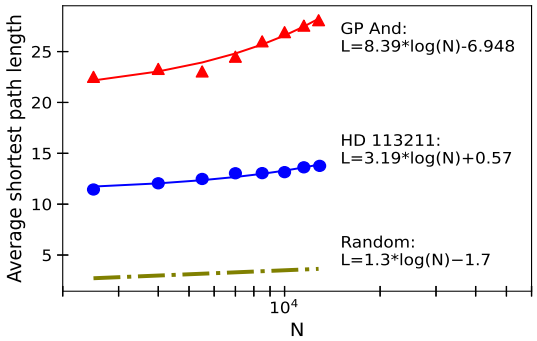

Figure 6. The relation between average shortest path length of the HVG network with the network sizes for HD 113211 (blue circles) and GP And star (red triangles). The fitted line for HD 113211 (blue line) and GP And star (red line) deviated from the random network (olive dash-dotted line).

at the light curve are connected to several neighboring small peaks and the other high peaks at the light curve. In the context of complex networks, reported a similar behavior for other small-world netwoks (Watts & Strogatz 1998; Mathias & Gopal 2001; Latora & Marchiori 2001).

Figure 7 depicts the scattering of the average clustering coefficients and transitivity of HVG networks for HADS (red triangles) and δ Sct (blue circles) stars. The HADS stars have high transitivity and low clustering coefficients, but δ Sct stars have different values. So, the HADS and δ Sct stars are clustered in two groups overlapping at some deals. The RX Cae (HD 28837) star (indicated by black arrow) was previously classified as a δ Sct star held out of regions for δ Sct stars group.

Figure 8 shows PDF and CCDF for nodes' degree of the HVG network for six HADS stars. As shown in the figure, the distribution of nodes degree is heavy-tail, so we fitted the power-law and lognormal distribution via the maximum likelihood estimation in the Bayesian framework (Section 3.2).

We observe that the peak of the nodes' degree distribution (Figure 8) for HADS (mono-periodic: GP And (TIC 436546358), CY Aqr (TIC 422412568), AD Cmi (HD 64191), and V367 Cam (TIC 354872568); double mode: V1384 Tau (TIC 415333069) and HD 146953) are precisely three or four. We analyzed the HVG characteristics of a single-mode artificial sinusoidal light curve to address this essential property of HADS stars. Figure 9 displays a part of the HVG network for a mono periodic artificial time series. We observe that the nodes with three links are more frequent than the others, with the number of connections differing from three. In other words, we follow that the nodes (black points) connect to three other nodes due to the behavior of a sinusoidal mono periodic artificial time series—this property of a fully sinusoidal time series with various frequencies/periods. However, most mono periodic stellar light curves have the HVG node distribution peaks of about three or four, similar to the artificial time series. However, the range of degree of nodes is different for a regular artificial time series and mono periodic stellar light curves. These differences may indicate the diverse nature of light curves of pulsating stars as κ, stochastic, or other complex generative mechanisms (Houdek et al. 1999; Samadi et al. 2002; Antoci et al. 2011; Antoci 2014) for pulsations from a regular sinusoidal oscillation. We find the p-value for both power-law fit and random model (Luque et al. 2009) is less than 0.01, which rejects both models for nodes' degree distribution of HADS stars. The rejection of the random model implies that the HADS and δ Sct stars light curve are not random. The p-values for lognormal fits are more than 0.1 (Table 1), which indicates we can not refute the lognormal model for nodes' degree distribution of HADS stars. We obtain the lognormal distribution parameters in the range of 3.05 to 3.86 and 0.2 to 0.6 for scale and shape, respectively. A lognormal distribution is due to a multiplicative process (e.g., Hubble 1934; Kolmogorov 1962; Miller & Scalo 1979; McBreen et al. 1994; Mouri et al. 2009). So, the lognormal behavior of nodes degree for stellar flux network may indicate the flux of HADS and δ Sct stars forming via some multiplicative process. Pauluhn & Solanki (2007) and Bazarghan et al. (2008) showed that the small-scale solar brightening features distribution follows a lognormal distribution.

Figure 10 shows PDF and CCDF for nodes' degree of the HVG network for six δ Sct stars HD 77914, HD 112063, HD 86312, HD 44930, HD 56843, and V479 Tau (HD 24550). Due to the tiny p-value (<0.01) for both the power-law fit and random model, we refute both models for nodes' degree distribution of δ Sct stars. We obtain the p-values more than 0.1 (Table 2) for lognormal fits, which shows we can not reject the lognormal model for nodes' degree distribution of δ Sct stars. We find the lognormal distribution parameters in the range of 2.4 to 3.9 and 0.33 to 0.6 for scale and shape, respectively.

Figure 11 depicts the CCDF of nodes' degree and PageRank of NVG network for HADS and δ Sct stars. We observe that both nodes' degree and PageRank distributions for HADS stars (red lines) are grouped above levels than the δ Sct (blue lines) stars. The high nodes' degree shows the significant number of connections of nodes with

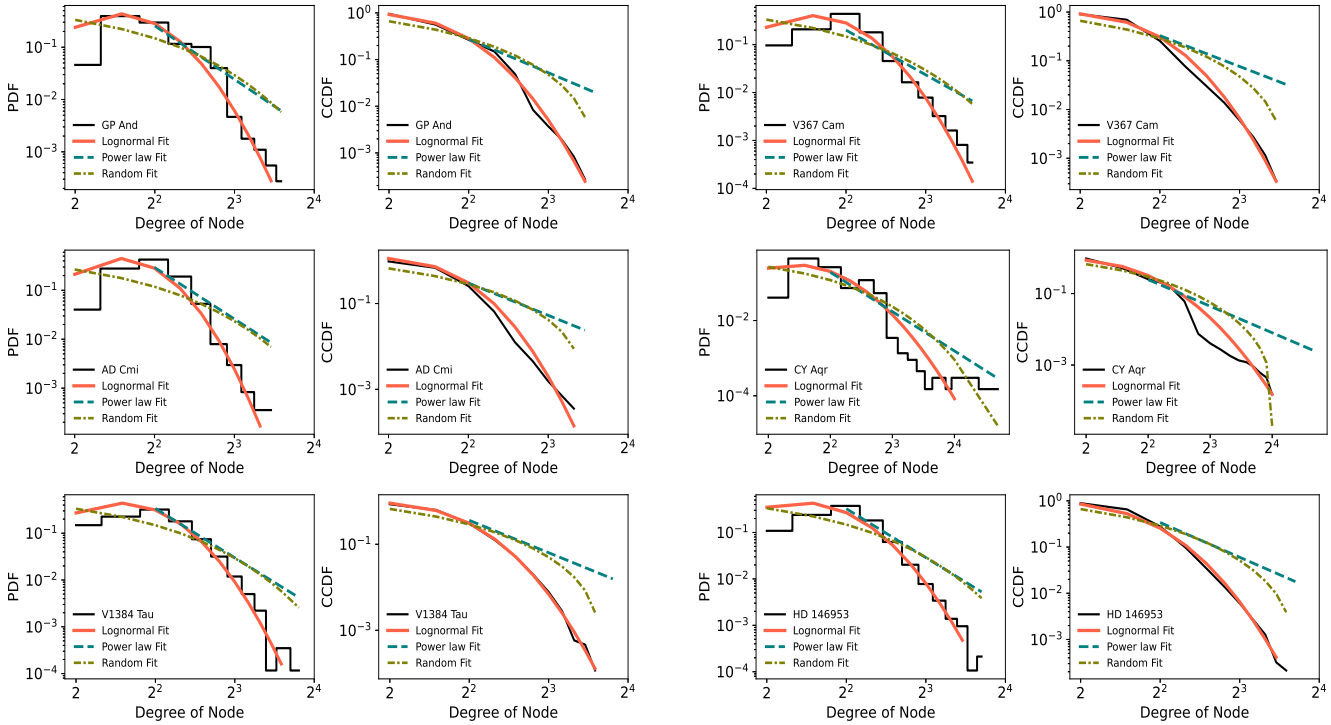

Figure 8. PDF and CCDF for the nodes degree of six HADS stars. Power laws (power law fit: blue dashed lines), lognormal functions (lognormal fit: red line) and random functions (random fit: olive dash-dotted) are fitted to each distribution.

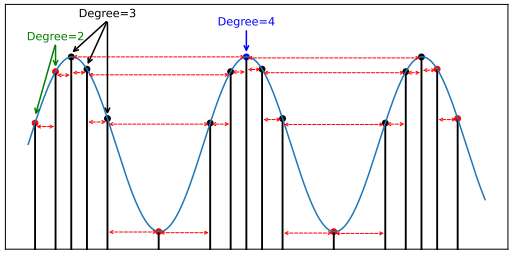

Figure 9. Schematic representation of a mono-periodic sinusoidal time series (light curve). The red double head arrows show the links of nodes via the HVG approach. The nodes with the color black, blue, and red have a degree of 3, 4, and 2, respectively. We ignored the network for analyzing two ends of the time series. Nodes with a degree of three are the most frequent.

others. However, the high PageRank indicates the important nodes or data points in the light curve with many in-links from other nodes. Since HADS are mostly mono-periodic or double mode stars, so high PageRank nodes (importance nodes) show a significant probability over the other nodes. However, due to the superposition of amplitudes of several modes for δ Sct stars, the high PageRanks (tail of the distribution) have low probability than the low PageRank.

Our analysis shows the ambiguity for CCDF (Figure 5) for light curves of RX Cae (HD 28837), V353 Vel (HD 93298), TIC 448892817, and GW Dra (TIC 329153513) samples of δ Sct stars. But our additional analysis of network properties (e.g., PageRank and nodes' degree distributions) indicates that the V353 Vel, TIC 448892817, and GW Dra stars are in the interface of HADS and δ Sct stars. More quantitative asteroseismological studies require identifying the exact property of these three stars. But, network properties for RX Cae suggest considering this star in the HADS subclass. Our frequency analysis for RX Cae shows several independent modes with amplitudes less than 0.3 mag in the power spectrum. The typical amplitude for the dominant mode of the HADS stars is more than 0.3 mag. Also, the dominant period (P = 0.15 d) and luminosity (M_V = 1.04 mag) for RX Cae satisfy the revised P-L realation $M_V = (2.94 \pm 0.06) \log P(1.34 \pm 0.06)$ (Ziaali et al. 2019).

5 CONCLUSIONS

We analyzed the PDF of short cadence flux light curves of 33 and 40 HADS and δ Sct stars (Table 1 and Table 2), respectively, observed by *TESS* mission. We show that the PDF of the flux of mono-periodic HADS stars has a similar shape to an analytical single-frequency periodic (sinusoidal) signal but deviates from analytical PDF relation at some deals due to some complexity at light curves (Figure 2). The PDF for light curves of double-mode HADS stars shows two close humps in a similar PDF for a time series as a superposition of two synthetic signals. The PDF of flux light curves for multi periodic δ Sct stars shows the normal like distributions and increasing the number of modes in the light curves the PDFs approach to normal standard distributions (Figure 3) with tiny differences at some deals may due to several factors like complexity behavior. We also find different behaviors (in the context of convex and concave functions) for CCDF of most HADS and δ Sct stars (Figure 5). We observed that the statistical behavior (PDF and CCDF) for amplitudes of synthetic time series is less sensitive to different white and red noise levels. However, more investigations on observational light curves need to be employed to accurately address the effect of the noises on the statistical behavior of observational light curves.

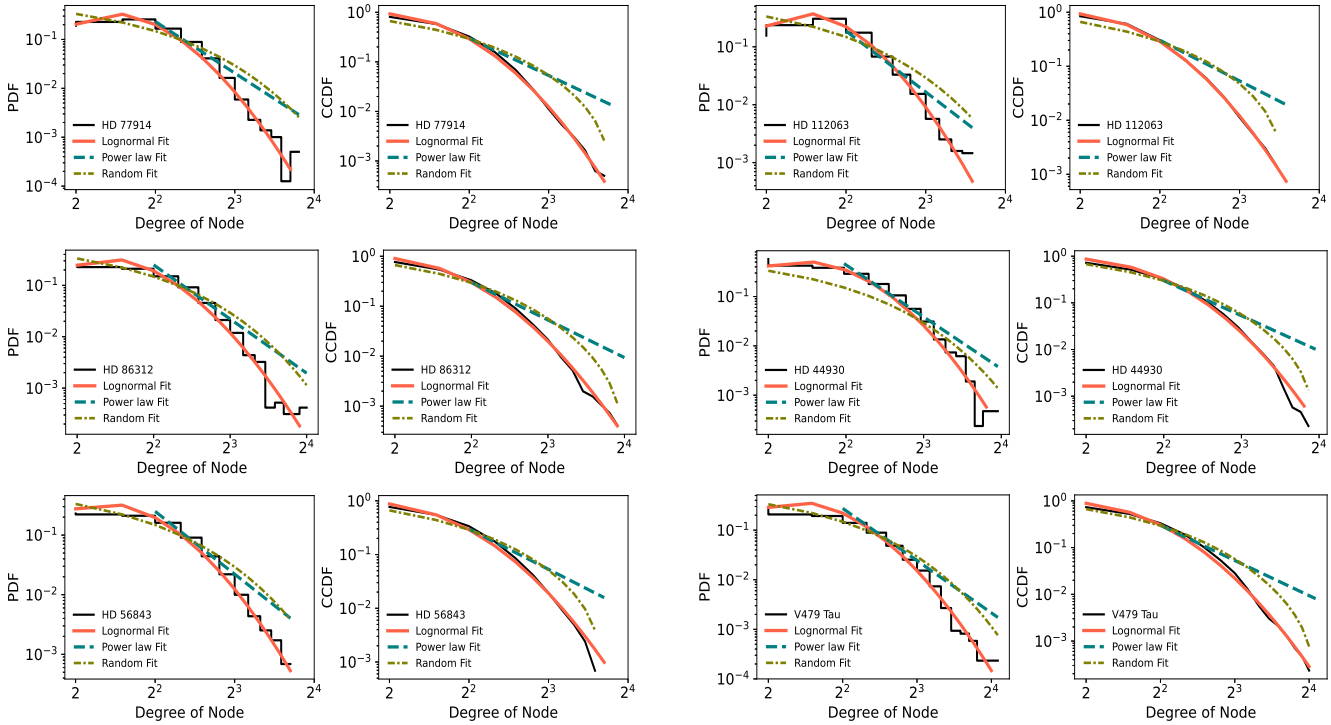

Figure 10. PDF and CCDF for the nodes degree of six δ Sct stars. Power laws (power law fit: blue dashed lines), lognormal functions (lognormal fit: red line) and random functions (random fit: olive dashdot) are fitted to each distribution.

The ambiguous behavior for some cases (e.g., V353 Vel (HD 93298)) may come from the binarity nature or other effects. Therefore, these differences in the shape of the PDF for light curves may be a helpful pre-estimation for number modes for mono-periodic, double modes, and multi-periodic oscillations, which may help the asteroseismology study of such stars. More quantitative statistics study requires investigating the effect of star rotation and other stellar quantities on the PDF of stellar flux light curves of HADS, δ Sct and other pulsating stars.

We investigate the network characteristics of HADS and δ Sct stars via the HVG and NVG algorithms, which both algorithms study the interaction of data points along the light curves (Figure 1). We focus on the network metrics that help to identify the HADS and δ Sct stars.

- The linear dependency of the average shortest path length (Figure 6) for HVG network size (in log space) of HADS and δ Sct stars indicates that the networks are small-world complex networks with non-random properties. This small-world property implies that the peaks of the stellar flux light curves connect with some small close peaks and are then linked to other significant peaks along the light curves.
- Scattering of transitivity and average clustering coefficient of HADS and δ Sct stars are clustered in two groups overlapping at some deals (Figure 7).
- The nodes' degree distribution of HVG networks (Figure 8 and 10) of HADS and δ Sct stars obey the lognormal distribution. The p-value of K-S statistics rejects both power-law and random network distribution. A lognormal behavior suggests a multiplicative generative mechanism for pulsating the HADS and δ Sct stars.
- We find that the nodes' degree and PangeRank distributions for NVG networks of HADS and δ Sct star are grouped in two classes for most cases (Figure 11).

Finally, we conclude that the statistics and network analysis of light curves are helpful for the asteroseismological studies (P-L relation, frequencies, etc.) of most HADS and δ Sct stars. However, the results of the present study suggest the RX Cae (HD 28837) as a HADS star, but the asteroseismological investigation studies identify it as a δ Sct star. Therefore, in most cases, the results of the present analysis via the statistics and complex network approach consist of asteroseismological findings. However, the statistics and complex network algorithms have much potential to investigate the physical and astrophysical characteristics of pulsating stars, e.g., from a complexity point of view. Also, more quantitative investigations need to be employed to study the effect of the noises on the global and local behavior of the complex networks for observational light curves of pulsating stars, which is our next logical step.

Table 1. Parameters and p-value of fitted lognormal distribution for HADS stars.

Star ID			Lognormal		
Name	HD	TIC	μ	σ	p-value
AD Cmi	64191	266328148	1.25 ± 0.08	0.29 ± 0.06	0.14
BE Lyn	79889	56914404	1.15 ± 0.07	0.45 ± 0.05	0.16
CY Aqr	–	422412568	1.19 ± 0.07	0.44 ± 0.06	0.18
DX Cet	16189	278962831	1.35 ± 0.06	0.33 ± 0.06	0.14
GP And	–	436546358	1.17 ± 0.07	0.35 ± 0.05	0.18
GW Uma	–	150276417	1.12 ± 0.07	0.44 ± 0.06	0.21
PT Com	–	335826251	1.19 ± 0.07	0.38 ± 0.06	0.28
RS Gru	206379	139845816	1.17 ± 0.06	0.46 ± 0.06	0.19
V 524 And	–	196562983	1.23 ± 0.08	0.33 ± 0.06	0.15
V367 Cam	–	354872568	1.27 ± 0.06	0.34 ± 0.04	0.19
V1162 Ori	–	34512862	1.30 ± 0.07	0.33 ± 0.04	0.21
V2455 Cyg	204615	266794067	1.25 ± 0.06	0.33 ± 0.06	0.17
YZ Boo	–	233465540	1.21 ± 0.07	0.37 ± 0.05	0.16
AN Lyn	–	56882581	1.32 ± 0.06	0.36 ± 0.05	0.20
–	146953	210548440	1.26 ± 0.06	0.35 ± 0.06	0.23
V1384 Tau	–	415333069	1.35 ± 0.06	0.32 ± 0.04	0.26
V1393 Cen	121517	241787384	1.24 ± 0.06	0.34 ± 0.05	0.20
V2855 Ori	–	166979292	1.32 ± 0.07	0.32 ± 0.05	0.22
ZZ Mic	199757	126659093	1.35 ± 0.06	0.27 ± 0.03	0.06
AE Uma	–	357132618	1.12 ± 0.07	0.43 ± 0.07	0.20
ρ Pup	67523	154360594	1.35 ± 0.06	0.21 ± 0.06	0.02
BL Cam	–	392774261	1.32 ± 0.06	0.37 ± 0.05	0.24
BS Aqr	223338	9632550	1.15 ± 0.08	0.39 ± 0.06	0.17
DE Lac	–	119486942	1.26 ± 0.07	0.38 ± 0.05	0.27
EH Lib	–	157861023	1.04 ± 0.08	0.42 ± 0.06	0.20
KZ Hya	94033	188209486	1.15 ± 0.07	0.39 ± 0.06	0.19
RY Lep	38882	93441696	1.28 ± 0.04	0.29 ± 0.02	0.08
SS Psc	–	456857185	1.36 ± 0.06	0.33 ± 0.05	0.32
SX Phe	223065	224285325	1.26 ± 0.06	0.35 ± 0.06	0.20
V1719 Cyg	200925	290277380	1.25 ± 0.04	0.30 ± 0.03	0.30
VX Hya	–	289711518	1.29 ± 0.05	0.40 ± 0.06	0.30
VZ Cnc	73857	366632312	1.17 ± 0.06	0.52 ± 0.06	0.21
XX Cyg	–	233310793	1.07 ± 0.07	0.45 ± 0.07	0.29

Table 2. Parameters and p-value of fitted lognormal distribution for δ Sct stars.

Star ID			Lognormal		
Name	HD	TIC	μ	σ	p-value
–	129831	81003	0.93 ± 0.09	0.47 ± 0.07	0.35
–	77914	975071	0.92 ± 0.09	0.47 ± 0.07	0.29
–	112063	9591460	0.89 ± 0.09	0.48 ± 0.07	0.29
RX Cae	28837	7808834	1.11 ± 0.07	0.34 ± 0.05	0.19
CV Phe	13755	7245720	1.17 ± 0.07	0.35 ± 0.05	0.32
–	21295	12524129	0.92 ± 0.09	0.58 ± 0.07	0.38
–	79111	18658256	0.88 ± 0.08	0.48 ± 0.06	0.35
–	86312	26957587	0.91 ± 0.08	0.52 ± 0.07	0.35
–	181280	30624832	0.89 ± 0.09	0.57 ± 0.07	0.38
–	44930	34737955	1.16 ± 0.07	0.45 ± 0.07	0.40
–	185729	79659787	0.91 ± 0.09	0.50 ± 0.08	0.33
–	25674	34197596	1.28 ± 0.07	0.41 ± 0.06	0.24
–	113221	102192161	0.97 ± 0.08	0.57 ± 0.08	0.42
–	180349	121729614	0.97 ± 0.09	0.57 ± 0.09	0.43
–	216728	137796620	0.91 ± 0.09	0.59 ± 0.08	0.38
–	113211	253296458	0.92 ± 0.08	0.58 ± 0.08	0.43
–	31322	246902545	1.31 ± 0.06	0.37 ± 0.05	0.28
–	32433	348792358	1.03 ± 0.08	0.48 ± 0.07	0.38
–	56843	387235455	0.97 ± 0.08	0.50 ± 0.07	0.38
–	38597	100531058	1.22 ± 0.07	0.41 ± 0.06	0.25
–	–	448892817	0.88 ± 0.08	0.49 ± 0.07	0.29
–	99302	458689740	0.97 ± 0.08	0.50 ± 0.07	0.41
V479 Tau	24550	459908110	0.98 ± 0.08	0.51 ± 0.07	0.39
V353 Vel	93298	106886169	1.21 ± 0.07	0.38 ± 0.06	0.29
–	17341	122615966	1.26 ± 0.06	0.41 ± 0.06	0.29
–	183281	137341551	1.13 ± 0.07	0.51 ± 0.07	0.32
–	182895	159647185	1.37 ± 0.07	0.42 ± 0.06	0.36
–	46722	172193026	1.28 ± 0.06	0.34 ± 0.04	0.24
–	8043	196921106	1.3 ± 0.06	0.46 ± 0.03	0.38
CC Gru	214441	161172103	0.87 ± 0.06	0.45 ± 0.06	0.16
–	24572	242944780	1.32 ± 0.06	0.41 ± 0.07	0.31
–	–	274038922	1.37 ± 0.06	0.34 ± 0.05	0.29
IN Dra	191804	269697721	1.29 ± 0.06	0.35 ± 0.05	0.31
GW Dra	–	329153513	1.31 ± 0.05	0.35 ± 0.05	0.27
CP Oct	21190	348772511	1.32 ± 0.06	0.33 ± 0.05	0.27
IO Dra	193138	403114672	1.34 ± 0.06	0.34 ± 0.05	0.31
–	42005	408906554	1.17 ± 0.07	0.46 ± 0.05	0.33
DE Cmi	67852	452982723	1.32 ± 0.06	0.34 ± 0.04	0.28
V435 Car	44958	255548143	1.32 ± 0.06	0.35 ± 0.05	0.32
V1790 Ori	290799	11361473	1.23 ± 0.07	0.45 ± 0.06	0.33

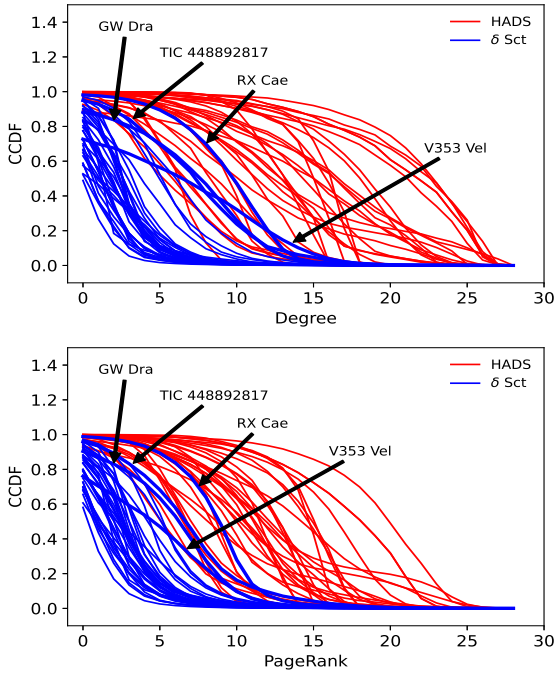

Figure 11. CCDF of nodes' degree (top panel) and PageRank (bottom panel) of NVG network for HADS (red lines) and δ Sct (blue lines) stars. The CCDF of nodes' degree and PageRank for RX Cae, V353 Vel, TIC 448892817, and GW Dra are samples that show different behavior of δ Sct stars.

ACKNOWLEDGEMENTS

This manuscript includes data collected by the TESS mission, which are publicly available from the Mikulski Archive for Space Telescopes (MAST). Funding for the TESS mission is provided by the NASA Explorer Program. Also, this work has been totally supported by the Iran National Science Foundation (INSF) under grant No. 4002562. E.Ziaali expresses her gratitude for that.

DATA AVAILABILITY

All Our codes and figures and tables will be shared on request to the corresponding author (safari@znu.ac.ir).

REFERENCES

Acosta-Tripailao B., Pastén D., Moya P. S., 2021, Entropy, 23, 470
Aerts C., 2021, Rev. Mod. Phys., 93, 015001
Aerts C., Thoul A., Daszynska J., Scuflaire R., Waelkens C., Dupret M.-A., Niemczura E., Noels A., 2003, Science, 300, 1926
Aerts C., Christensen-Dalsgaard J., Kurtz D., 2010, Asteroseismology. Astronomy and Astrophysics Library, Springer Netherlands, https://books.google.com/books?id=N8pswDrdSyUC
Alipour N., et al., 2022, A&A, 663, A128
Antoci V., 2014, in Guzik J. A., Chaplin W. J., Handler G., Pigulski A., eds, Vol. 301, Precision Asteroseismology. pp 333–340 (arXiv:1311.1149), doi:10.1017/S1743921313014543
Antoci V., et al., 2011, Nature, 477, 570
Antoci V., et al., 2014, ApJ, 796, 118
Antoci V., et al., 2019, Monthly Notices of the Royal Astronomical Society, 490, 4040
Audenaert J., et al., 2021, AJ, 162, 209
Baglin A., 2003, Advances in Space Research, 31, 345
Baglin A., Auvergne M., Barge P., Deleuil M., Michel E., CoRoT Exoplanet Science Team 2009, in Pont F., Sasselov D., Holman M. J., eds, Vol. 253, Transiting Planets. pp 71–81, doi:10.1017/S1743921308026252
Baiesi M., Paczuski M., 2004, Phys. Rev. E, 69, 066106
Balona L. A., 2016, MNRAS, 459, 1097
Balona L. A., 2018, MNRAS, 479, 183
Balona L., Dziembowski W., 2011, Monthly Notices of the Royal Astronomical Society, 417, 591
Balona L. A., et al., 2012, MNRAS, 419, 3028
Barabasi A.-L., Oltvai Z. N., 2004, Nature reviews genetics, 5, 101
Barac N., Bedding T. R., Murphy S. J., Hey D. R., 2022, MNRAS,
Barbara N. H., Bedding T. R., Fulcher B. D., Murphy S. J., Van Reeth T., 2022, MNRAS, 514, 2793
Barclay T., Pepper J., Quintana E. V., 2018, ApJS, 239, 2
Basu S., Chaplin W., 2017, Asteroseismic Data Analysis: Foundations and Techniques. Princeton Series in Modern Observational Astronomy, Princeton University Press, https://books.google.de/books?id=IGuYDwAAQBAJ
Bazarghan M., Safari H., Innes D. E., Karami E., Solanki S. K., 2008, A&A, 492, L13
Bedding T. R., et al., 2020, Nature, 581, 147
Bowman D. M., 2017, Amplitude Modulation of Pulsation Modes in Delta Scuti Stars, doi:10.1007/978-3-319-66649-5.
Bowman D. M., Kurtz D. W., 2018, MNRAS, 476, 3169
Bowman D. M., Kurtz D. W., Breger M., Murphy S. J., Holdsworth D. L., 2016, MNRAS, 460, 1970
Bowman D., Hermans J., Daszyńska-Daszkiewicz J., Holdsworth D. L., Tkachenko A., Murphy S., Smalley B., Kurtz D. W., 2021a, Monthly Notices of the Royal Astronomical Society, 504, 4039
Bowman D., Hermans J., Daszyńska-Daszkiewicz J., Holdsworth D. L., Tkachenko A., Murphy S., Smalley B., Kurtz D. W., 2021b, Monthly Notices of the Royal Astronomical Society, 504, 4039
Breger M., 2000, in ASP Conf. Series, Vol. 210. p. 3
Campante T. L., et al., 2016, ApJ, 830, 138
Chang S.-W., Protopapas P., Kim D.-W., Byun Y.-I., 2013, Astron. J., 145, 132
Chaplin W. J., Houdek G., Karoff C., Elsworth Y., New R., 2009, A&A, 500, L21
Chaplin W. J., et al., 2020, Nature Astronomy, 4, 382
Christensen-Dalsgaard J., 2004, in Danesy D., ed., ESA Special Publication Vol. 559, SOHO 14 Helio- and Asteroseismology: Towards a Golden Future. p. 1
Clauset A., Shalizi C. R., Newman M. E. J., 2009, SIAM Review, 51, 661
Cox J. P., 1963, The Astrophysical Journal, 138, 487
Daei F., Safari H., Dadashi N., 2017, ApJ, 845, 36
Eddington A., 1919, Monthly Notices of the Royal Astronomical Society, 79, 177
Farhang N., Safari H., Wheatland M. S., 2018, ApJ, 859, 41
Farhang N., Shahbazi F., Safari H., 2022, arXiv e-prints, p. arXiv:2208.02493
Feinstein A. D., et al., 2019, PASP, 131, 094502
Gheibi A., Safari H., Javaherian M., 2017, ApJ, 847, 115
Gilliland R. L., et al., 2010, PASP, 122, 131
Handler G., 2013, in Oswalt T. D., Barstow M. A., eds, , Vol. 4, Planets, Stars and Stellar Systems. Volume 4: Stellar Structure and Evolution. p. 207, doi:10.1007/978-94-007-5615-1_4
Hasanzadeh A., Safari H., Ghasemi H., 2021, MNRAS, 505, 1476
Herrero E., Morales J. C., Ribas I., Naves R., 2011, A&A, 526, L10
Houdek G., Balmforth N. J., Christensen-Dalsgaard J., Gough D. O., 1999, A&A, 351, 582
Hubble E., 1934, ApJ, 79, 8
Jayasinghe T., et al., 2020, Monthly Notices of the Royal Astronomical Society, 493, 4186
Kahraman Aliçavuş F., Niemczura E., Polińska M., Hełminiak K. G., Lampens P., Molenda-Żakowicz J., Ukita N., Kambe E., 2017, MNRAS, 470, 4408
Kahraman Aliçavuş F., Gümüş D., Kırmızıtaş Ö., Ekinci Ö., Çavuş S., Kaya Y. T., Aliçavuş F., 2022, Research in Astronomy and Astrophysics, 22, 085003
Kolmogorov A. N., 1962, Journal of Fluid Mechanics, 13, 82
Kurtz D., 2022, in Annual Conference and General Assembly of the African Astronomical Society. p. 1 (arXiv:2201.11629)
Latora V., Marchiori M., 2001, Phys. Rev. Lett., 87, 198701
Lee J. W., Hong K., Kristiansen M. H., 2020, Publications of the Astronomical Society of Japan, 72, 37
Liakos A., Niarchos P., 2017, MNRAS, 465, 1181
Lotfi N., Javaherian M., Kaki B., Darooneh A. H., Safari H., 2020, Chaos, 30, 043124
Lund M. N., et al., 2021, The Astrophysical Journal Supplement Series, 257, 53
Luque B., Lacasa L., Ballesteros F., Luque J., 2009, Physical Review E, 80, 046103
Mathias N., Gopal V., 2001, Phys. Rev. E, 63, 021117
McBreen B., Hurley K. J., Long R., Metcalfe L., 1994, MNRAS, 271, 662
McNamara D. H., 2011, AJ, 142, 110
McNamara D. H., Clementini G., Marconi M., 2007, AJ, 133, 2752
Michel E., et al., 2017, in EPJWC. p. 03001 (arXiv:1705.03721)
Miller G. E., Scalo J. M., 1979, ApJS, 41, 513
Mohammadi Z., Alipour N., Safari H., Zamani F., 2021, Journal of Geophysical Research (Space Physics), 126, e28868
Mouri H., Hori A., Takaoka M., 2009, Physics of Fluids, 21, 065107
Murphy S. J., Saio H., Takada-Hidai M., Kurtz D. W., Shibahashi H., Takata M., Hey D. R., 2020, Monthly Notices of the Royal Astronomical Society, 498, 4272
Najafi A., Darooneh A. H., Gheibi A., Farhang N., 2020, ApJ, 894, 66
Newman M. E., 2003, SIAM review, 45, 167
Newman M., 2010, Networks: An Introduction. OUP Oxford, https://books.google.de/books?id=-DgTDAAAQBAJ
Niemczura E., et al., 2015, Monthly Notices of the Royal Astronomical Society, 450, 2764

Pakštienė E., Janulis R., Tautvaišienė G., Drazdauskas A., Klebonas L., Mikolaitis Š., Minkevičiūtė R., Bagdonas V., 2018, PASP, 130, 084201
Pamyatnykh A. A., 2000, in Breger M., Montgomery M., eds, Astronomical Society of the Pacific Conference Series Vol. 210, Delta Scuti and Related Stars. p. 215 (arXiv:astro-ph/0005276)
Pastén D., Czechowski Z., Toledo B., 2018, Chaos, 28, 083128
Pauluhn A., Solanki S. K., 2007, A&A, 462, 311
Poretti E., 2003, A&A, 409, 1031
Pribulla T., Kreiner J., Tremko J., 2003, Contributions of the Astronomical Observatory Skalnate Pleso, 33, 38
Qian S.-B., Li L.-J., He J.-J., Zhang J., Zhu L.-Y., Han Z.-T., 2018, MNRAS, 475, 478
Ricker G. R., et al., 2015, Journal of Astronomical Telescopes, Instruments, and Systems, 1, 014003
Rodríguez E., López-González M. J., López de Coca P., 2000, A&AS, 144, 469
Rucinski S. M., 2007, MNRAS, 382, 393
Samadi R., Goupil M. J., Houdek G., 2002, A&A, 395, 563
Silva Aguirre V., et al., 2015, MNRAS, 452, 2127
Souma W., Fujiwara Y., Aoyama H., 2003, Physica A Statistical Mechanics and its Applications, 324, 396
Stassun K. G., et al., 2018, AJ, 156, 102
Sullivan P. W., et al., 2015, ApJ, 809, 77
Taran S., Khodakarami E., Safari H., 2022, Advances in Space Research
Uytterhoeven K., et al., 2011, Astronomy & Astrophysics, 534, A125
Vogel E. E., Brevis F. G., Pastén D., Muñoz V., Miranda R. A., Chian A. C.-L., 2020, Natural Hazards and Earth System Sciences, 20, 2943
Watts D. J., Strogatz S. H., 1998, Nature, 393, 440
Yang T.-Z., Zuo Z.-Y., Sun X.-Y., Tang R.-X., Esamdin A., 2022, ApJ, 936, 48
Ziaali E., Bedding T. R., Murphy S. J., Van Reeth T., Hey D. R., 2019, MNRAS, 486, 4348

This paper has been typeset from a TEX/LATEX file prepared by the author.